

Article

Performance Characteristics of a Dual-Stator, Spoke-Type Permanent Magnet Vernier Machine with Support Bar

Jang-Hyun Park ¹, Grace Firsta Lukman ¹, Do-Hyun Kang ^{2,*} and Jin-Woo Ahn ¹

¹ Department of Mechatronics Engineering, Kyungsoong University, Busan 48434, Korea; jhpark7@kakao.com (J.-H.P.); gracedr@ks.ac.kr (G.F.L.); jwahn@ks.ac.kr (J.-W.A.)

² VAM, Inc., Changwon 51542, Korea

* Correspondence: dowajuge@gmail.com; Tel.: +82-(0)10-3582-7056

Abstract: Permanent magnet Vernier machine (PMVM) is a strong candidate for direct-drive applications in low-speed region because its power characteristic is higher than conventional permanent magnet machine (PMM). In this paper, the design of a dual-stator PMVM (DSPMVM) with spoke-type rotor is introduced. As a radial motor with dual-stator configuration, one on the outer and inner side, the rotor is equipped with support bars for practical and simple manufacturing, which is the aim of this study. The characteristics and performance of the proposed machine with and without the support bar are examined with finite element analysis (FEA). The DSPMVM and the support were manufactured and tested through experiments to verify proposed structure. Both simulation and experiment results show that there is little to no difference in performance when the support bar is equipped. Furthermore, the average deviation between simulation and experiment results is approximately 7% which is within the acceptable range.

Keywords: dual-stator permanent magnet Vernier machine; dual air gap; spoke array rotor



Citation: Park, J.-H.; Lukman, G.F.; Kang, D.-H.; Ahn, J.-W. Performance Characteristics of a Dual-Stator, Spoke-Type Permanent Magnet Vernier Machine with Support Bar. *Energies* **2021**, *14*, 1068. <https://doi.org/10.3390/en14041068>

Academic Editor: Federico Barrero

Received: 3 February 2021
Accepted: 16 February 2021
Published: 18 February 2021

Publisher's Note: MDPI stays neutral with regard to jurisdictional claims in published maps and institutional affiliations.



Copyright: © 2021 by the authors. Licensee MDPI, Basel, Switzerland. This article is an open access article distributed under the terms and conditions of the Creative Commons Attribution (CC BY) license (<https://creativecommons.org/licenses/by/4.0/>).

1. Introduction

In recent years, low-speed high-power rotating machines have been gaining more attention for direct-drive applications such as electric propulsion, wind generator, industrial robots, washing machines, etc. However, the currently existing machines in the market are required to produce low-speed and high-power characteristics. As a result, a considerable amount of materials are needed and the machines are also heavy.

Permanent magnet Vernier machine (PMVM) is a magnetically geared machine whose operation is based on the magnetic gearing effect through flux modulation poles (FMPs). The machine is derived from the earlier Vernier reluctance machine [1]. Because of the magnetic gearing effect, PMVM has high-power characteristic [2,3]. Various literatures show that PMVM can be a viable option for size and cost reduction. The output power can reach almost three times of an equivalent conventional PMM for the same current and volume [4]. However, unlike PMM, PMVM is usually designed and operated at much lower rotation speed because of the large magnet pole number [5].

It is well-known that air gap stores most of the energy, and thus, the dual-stator (DS) structure can be adopted to further increase the torque density. The effective space utilization with dual air gap on the outer and inner side of the rotor makes it possible to generate even more torque for a given volume [6–8]. A problem with DS machines is the complicated mechanical configuration of the rotor.

Spoke-type rotor is a common configuration used in permanent magnet machines. The advantage of this configuration is that high air-gap flux density can be obtained because of the flux focusing effect [9]. However, because of the dual stator structure, the implementation of the conventional spoke array is difficult, since the rotor cannot be connected to the shaft directly. A solution to this problem is to use an additional rotor frame with a bridge layer that wraps the rotor surface as was introduced in [10]. However, this

adds unnecessary length to the air-gap length and thus is not suitable if the development goal is a compact machine with high torque density. A literature in [11] also proposed a frame configuration to hold the rotor. It involved two shafts, one for the inner stator and one for the rotor. This structure requires precise manufacturing to properly balance the rotor support frame and both stators.

In this paper, a DSPMVM with spoke-type rotor and a stainless-steel support bar are proposed. Few literatures already discussed about DSPMVM, but they are focused on the characteristics of the motor, ignoring the difficulty in manufacturing process. This paper focuses on manufacturing practicability and motor compactness and ruggedness. Instead of using a full cover for the rotor, four bars in place of the four spoke arrays are used to hold the rotor. Since the proposed support replaces some parts of the core, finite element analysis (FEA) is used to examine the difference between the rotor with and without support in terms of average torque, torque ripple, and cogging torque. To verify the validity of the analysis, the proposed DSPMVM was manufactured and tested.

2. Operating Principle of Permanent Magnet Vernier Machines

Figure 1 shows the linear-equivalent geometry of a conventional PMVM. In the figure, the rotor is rotating in a counterclockwise direction, and the arrows indicate the polarity of the magnets. θ and θ_m are the mechanical angle of stator and the rotor position angle.

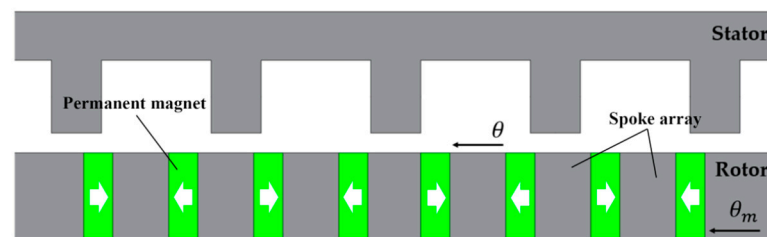


Figure 1. Illustration of permanent magnet Vernier machine (PMVM) geometry.

PMVM uses the concept of magnetic gearing effect in the air gap. In order to obtain this effect, PMVM design must satisfy the following relationship [5]:

$$Z_r = Z_s \pm p \quad (1)$$

where Z_r , Z_s , and p are the number of pole pair of rotor PM, stator teeth, and stator pole pairs, respectively. In addition, operating principle of PMVM can be explained by the air gap permeance function. This function can be written as a Fourier series as follows,

$$P(\theta) = P_0 + \sum_{m=1}^{\infty} P_m \cos(mZ_s\theta) \quad (2)$$

where P_0 is an average air gap permeance coefficient and P_m is the amplitude of the permeance coefficient according to the harmonic order. As the rotor rotates, the rotor magnets generate MMF according to Z_r pole pairs. The gap between the stator teeth creates a change of air gap as the rotor rotates and “modulates” the gap permeance due to the flux modulation effect. Air gap magnetomotive force (MMF) from permanent magnet of rotor can also be expressed in Fourier series as follows,

$$F_{gap}(\theta) = \frac{4}{\pi} F_{gap} \sum_{n=1,3,5\dots}^{\infty} \frac{1}{n} \cos\{nZ_r(\theta - \theta_m)\} \quad (3)$$

where F_{gap} is average value of air-gap MMF.

The magnetic flux density of the DSPMVM can also be defined using the air gap permeance function, which only considers the major or $m = 1$ and $n = 1$ components. Thus, the no-load magnet flux density of air gap $B_{PM}(\theta)$ is expressed as follows,

$$B_{PM}(\theta) = F_{gap}(\theta)P(\theta) = B_1 + B_2 + B_{har} \tag{4}$$

$$B_1 = B_{PM0} \cos(Z_r(\theta - \theta_m)) \tag{5}$$

$$B_2 = B_{PM1} \cos((Z_r - Z_s)\theta - Z_r\theta_m) \tag{6}$$

where $B_{PM0} = \frac{4}{\pi}F_{gap}P_0$, $B_{PM1} = \frac{2}{\pi}F_{gap}P_1$, and B_{har} is the harmonic component. Equation (5) is merely a product of P_0 and the fundamental component of air gap MMF from the PM rotor. However, in (6), the period is modulated by its relationship with Z_r and Z_s , that creates the magnetic gearing effect in the air gap. Therefore, a small change of rotor position angle can generate higher speed change than (5).

3. Configuration of the Dual-Stator Permanent Magnet Vernier Machine

Figure 2 shows the proposed structure of the DSPMVM. The two stators are each located at the outer and the inner part of the rotor with the rotor placed in the middle. Concentrated winding is selected to generate MMF with three-phase sinusoidal AC as the input. The rated speed is 600 RPM and the total input current is 6120 ampere-turn (AT). The windings of the proposed DSPMVM for both stators are connected in series according to the Y-connection topology as shown in Figure 3. Therefore, instead of two, only one converter is required to operate the DSPMVM, similar to single-stator machines. Table 1 shows the detail of the physical specifications of the proposed machine [12].

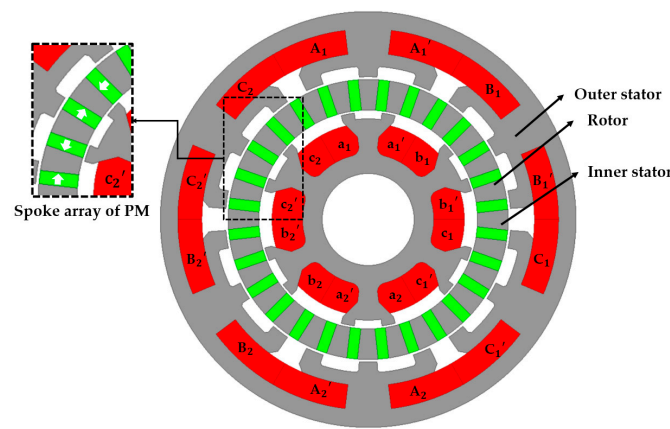


Figure 2. Geometry of the dual-stator permanent magnet Vernier machine (DSPMVM).

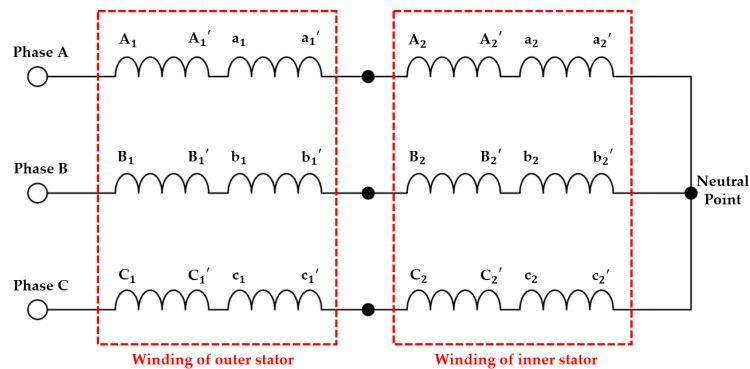


Figure 3. Winding connection of the DSPMVM machine.

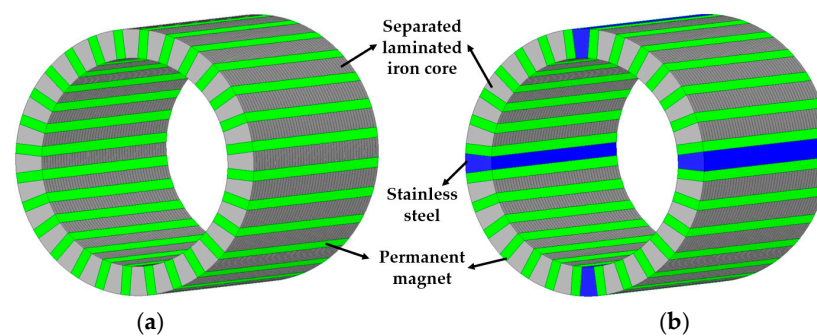
Table 1. Main specifications of the DSPMV machine.

Description	Value
Outer diameter of outer stator (mm)	95
Outer diameter of rotor (mm)	64
Outer diameter of inner stator (mm)	60
Stack length (mm)	55
Outer air gap (mm)	0.6
Inner air gap (mm)	0.5
Core material	35PN380
Permanent magnet material	NdFeB – Br = 1.2 T; $\mu_r = 1.04$ at 20 °C
Total current ampere-turn (100%) (rms current per slot \times number of slot)	6120 AT (255 \times 24)

The DSPMVM has flux-modulation poles (FMPs), three FMPs on outer stator and two FMPs on inner stator. FMPs divide the MMF produced by the stator winding, transfer them to the air gap, and the modulated magnetic field then synchronizes this MMF with the rotor magnet MMF. Therefore, FMP is a major factor that determines the magnetic gearing effect [2,3].

4. Proposed Rotor Structure

The conventional spoke-type rotor with no support is shown in Figure 4a. Without support, it is difficult to practically use the machine because the mechanical connection between the rotating part to the shaft or direct application is not available.

**Figure 4.** Structure of rotors. (a) With no support. (b) With proposed support-bar.

In this paper, a simple support bar made from stainless steel is simply inserted to replace four spoke arrays with the interval of 90 degrees each to hold the rotor, as shown in Figure 4b. The iron core for the spokes is laminated in a way that any rotor core does, but the stainless steel is a solid part. Therefore, there will be no difficulties in the welding or assembly process of the support bar with the support frame. In this section, the effect of the proposed support bar is examined [13].

Stainless steel belongs to the group of alloys, and it can be classified into austenite, duplex, ferrite, and martensite based on its chemical composition and metal tissue. Stainless steel grade 304 (SUS304) of austenite and grade 430 of ferrite with the resistance to corrosion that are commonly used in industrial are selected. However, SUS304 has non-magnetic flow property whereas SUS430 which has magnetic property. Thus, the magnetic flow through SUS304 is low because its relative permeability of this material is 1 like that of the air. Theoretically, to guarantee the magnetic flow path in the rotor, SUS430 has to be selected as the material for the support bar [14]. For comparison, the three materials are first compared. The magnetization curve comparison between the iron core material 35PN380, SUS430, and SUS304 is shown in Figure 5 below.

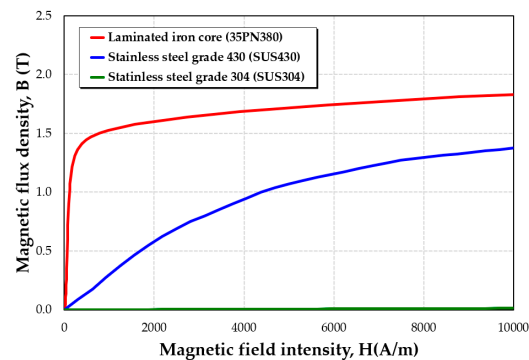


Figure 5. Magnetization curve of 35PN380, SUS304, and SUS430.

5. FEA Simulation Results

The electromagnetic characteristics are analyzed through FEA simulation using Ansys Electronics Desktop. Torque characteristics, which consists of average torque, torque ripple, and cogging torque, are considered as comparison parameters for rotor with and without support.

Figure 6 shows the magnetic field density in the machine. Type 1 is the rotor without support bar, Type 2 is the rotor with support bar of SUS304 material, and Type 3 is the rotor with SUS430 as the material for the bar. As previously mentioned, Type 2 rotor result is the same as removing the spoke arrays, and not replacing it as no magnetic flux can flow through the bar because the permeability of SUS304 is like that of the air. However, the field density of Type 1 and 3 is similar, indicating that there will be little to no effect on performance if four spoke arrays are replaced with the SUS430 bars, which have magnetic property.

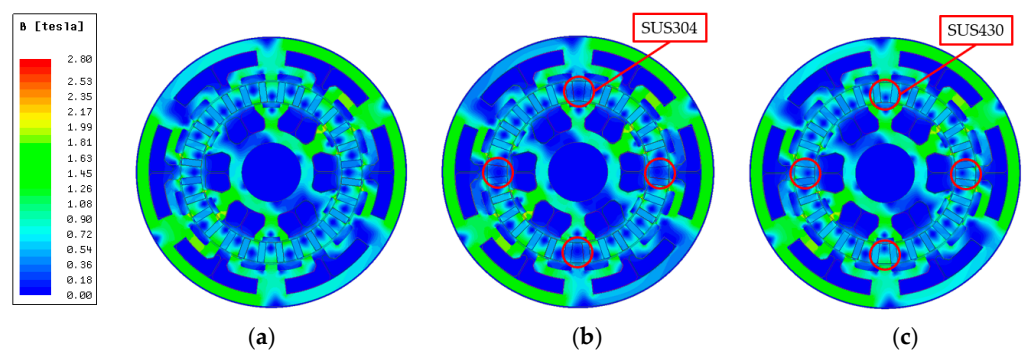


Figure 6. Magnetic field density: (a) Type 1, (b) Type 2, and (c) Type 3.

Torque characteristics comparison is presented in Table 2 and Figure 7. From the explanation above, it is as expected that Type 2 cannot satisfy the performance requirement. As for Type 1 and 3, the average torque generated by the proposed machine with support bar with SUS430 is merely decreased by 0.3%. In the case of torque ripple and cogging torque, there are increases of 32% and 4.7%, respectively, with the proposed structure of SUS430.

Table 2. Torque characteristics comparison of the proposed DSPMVM.

Description	Type 1 (no Support)	Type 2 (SUS304)	Type 3 (SUS430)
Average torque (Nm)	13.28	11.23	13.26
Torque ripple (%)	1.68	15.03	2.06
Cogging torque (Nm)	0.43	2.31	0.47

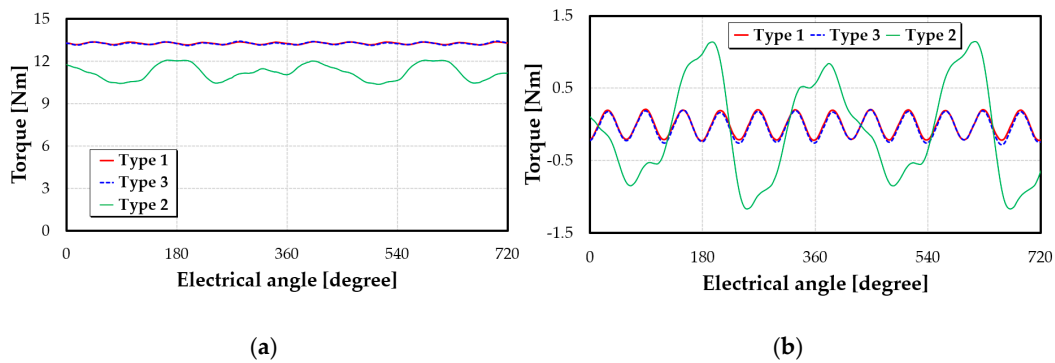


Figure 7. Torque characteristics: (a) torque and (b) cogging torque.

6. Experimental Validation

The conventional spoke-type rotor without the bar makes it very difficult to connect the rotor with the support frame. Therefore, the proposed structure uses four solid bars from stainless steel to connect to the frame. Using this method, manufacture is easy, and the rotor can be firmly held during rotation. Figure 8 shows the overall structure of the frame. The connection with each SUS430 bar and the support frame is joined by welding. Unlike the conventional structure of single-stator machines, the proposed DSPMVM only has a single-sided shaft. Compared to the structure proposed in [11], the stators of proposed PMVM are joined together on the side without shaft and rotor is fixed to the stators with bearings [13].

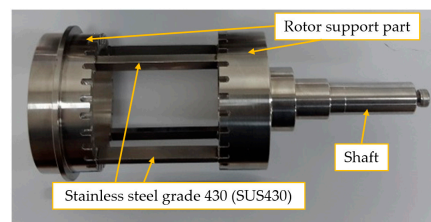


Figure 8. Rotor of proposed type.

The validation through experiment is achieved by static characteristic experiment. and the setup is shown in Figure 9. A 1/100 reducer is used to rotate the rotor, and one rotation of the knob is equal to the rotor rotation of 3.6 degrees. The two power supplies are used to provide a wide range of input current because one can supply 6 A and the other 10 A as the maximum supply current. Therefore, input current 16 A as the maximum current can be supplied to DSPMVM by the parallel connection of power supplies.

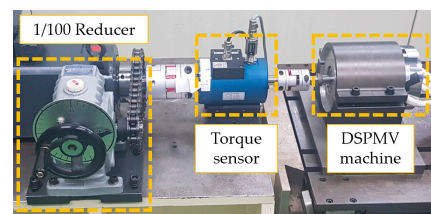


Figure 9. Experimental setup.

The experiment process to measure the static characteristic experiment is very simple. The rotating magnetic field of stators is pre-set, and the rotor is rotated with a reducer manually using the knob. Using this method, the static characteristic profile can be measured in the accuracy of one electrical angle. The advantage of the static characteristic experiment is that it is possible to check whether the manufactured machine complies with the design

or not. Moreover, this experiment can predict the maximum torque values in dynamic experiment by doing the measurement for each load current.

A specific point in three-phase sinusoidal AC is decided as the injection current to the DSPMVM which generates the fixed rotating magnetic field. Three-phase sinusoidal AC are expressed as,

$$i_{a,b,c}(t) = \sqrt{2}I_{rms} \sin(\omega t + \alpha) \quad (7)$$

where, I_{rms} is the rms value of current, and α is the phase difference. In order to simplify the experiment, the zero-time point of three-phase sinusoidal AC is selected, and thus, $i_a(0) = 0$, $i_b(0) = -\sqrt{6}/2I_{rms}$, and $i_c(0) = \sqrt{6}/2I_{rms}$ according to Equation (7). Therefore, it is possible to generate the rotating magnetic field by injecting only single-phase DC current with the power supplies. Then, while rotating the reducer, static characteristic profile of the DSPMVM can be obtained for one electrical cycle. The diagram of static characteristic experiment is shown in Figure 10. Figure 11 shows the static characteristic profiles of input current 50% and 100% input current for one electrical cycle.

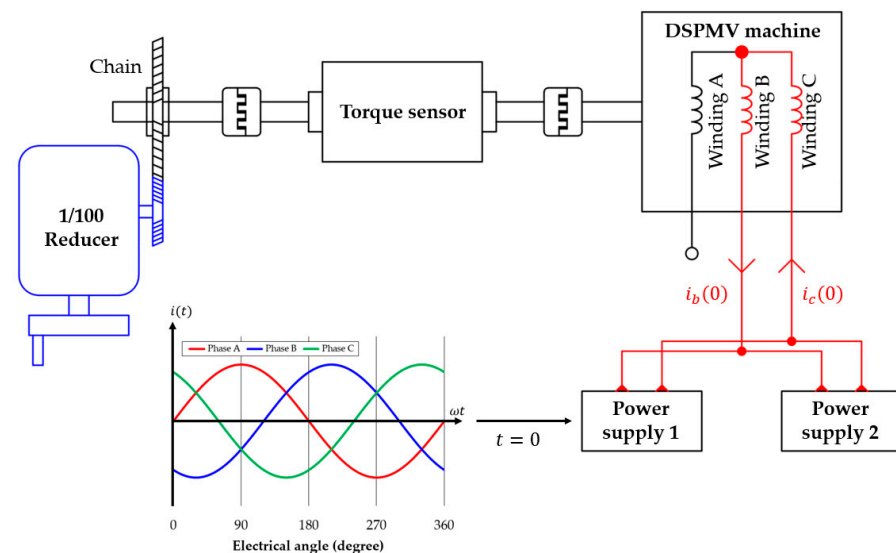


Figure 10. Diagram of static characteristic experiment.

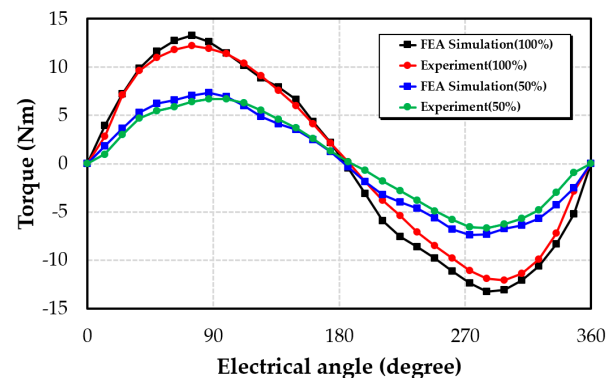


Figure 11. Static characteristic profiles for one electrical angle.

Figure 12 and Table 3 show the maximum torque value comparison between the FEA simulation and experiment when the ampere-turn of input current ampere turn is increased from 0% to 150% considering only the positive torque region. The average deviation of the maximum torque between the two result groups is approximately 7%. This suggests that the manufactured machine complies with the design. Furthermore, the FEA result in Table 3 is nearly equal to the dynamic torque value as shown Table 2. Therefore, it can be estimated that the actual dynamic torque will also follow that of the simulation.

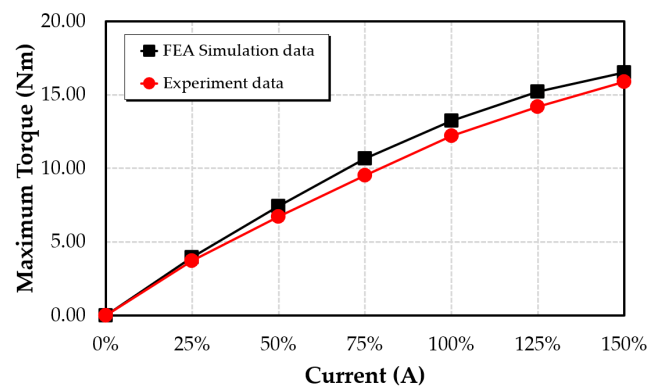


Figure 12. Maximum torque for different input currents.

Table 3. Torque characteristics comparison between simulation and experiment.

Input Current (%)	Maximum Torque (Nm)	
	FEA Simulation	Experiment
0%	0.0	0.0
25%	3.9	3.7
50%	7.4	6.7
75%	10.6	9.5
100%	13.2	12.2
125%	15.2	14.2
150%	16.5	15.9

The comparison between the DSPMVM with conventional PMM is shown in Table 4. Tangential force, which is responsible for torque production, per rotor area can be calculated as follows [15]:

$$F_{td} = \frac{\text{Tangential force}}{\text{Rotor surface area}} = \frac{T}{2\pi r^2 L_{st}} \quad (8)$$

where T , r , and L_{st} are torque, outer radius of the rotor, and stack length, respectively. The tangential force is 436% higher than that of the PMM. This result shows the viability to use the proposed machine for low-speed, high-power applications.

Table 4. Comparison of the proposed DSPMVM with conventional PMM.

Description	DSPMVM	Conventional PMM
Total current ampere-turn (AT)	6120	←
Outer diameter of stator (mm)	95	100
Outer diameter of rotor (mm)	64	63.5
Stack length (mm)	55	31
Air gap (mm)	0.5/0.6	0.8
Volume (L)	0.39	0.24
Rated speed (RPM)	600	1800
Rated torque (Nm)	12.2	1.57
Output power (W)	766	295
Volumetric torque density (Nm/L)	31.28	6.54
Tangential force per rotor area (kN/m ²)	34.5	7.9

7. Conclusions

In this paper, a dual-stator permanent magnet Vernier machine (DSPMVM) with a spoke-type rotor and rotor support bar is proposed. The DSPMVM generates high torque density but is structurally complex, which can make manufacturing difficult. Therefore, four support bars as a replacement of four spoke arrays are proposed. The bars are solid and not laminated, and so it is easy to connect to the support frame. The proposed DSPMVM

was successfully manufactured without any particular difficulty. The experimental results match with simulation within the allowable error tolerance. Therefore, it can be concluded that replacing four spoke arrays with bars made of SUS430 of stainless-steel material has a small effect on the performance, and the motor retains its characteristics. Moreover, the dynamic characteristics can be estimated from the static experiment. Compared to a conventional PMM, the proposed motor is 478% higher in Volumetric torque density and 436% higher in tangential force per rotor area. The dynamic performance parameters such as efficiency, power factor, and speed-torque curve are not studied in this paper and will be added in future works.

Author Contributions: Conceptualization, D.-H.K.; manufacturing, D.-H.K.; software, J.-H.P.; validation; J.-H.P.; writing—original draft preparation, J.-H.P.; writing—review and editing, G.F.L.; supervision, J.-W.A. All authors have read and agreed to the published version of the manuscript.

Funding: This work was partially supported by “Human Resources Program in Energy Technology” of the Korea Institute of Energy Technology Evaluation and Planning (KETEP), granted financial resource from the Ministry of Trade, Industry & Energy, Republic of Korea. (No. 20184010201700).

Institutional Review Board Statement: Not applicable.

Informed Consent Statement: Not applicable.

Data Availability Statement: Not applicable.

Acknowledgments: This research was conducted with VAM, Inc.

Conflicts of Interest: The authors declare no conflict of interest.

References

1. Lee, C.H. Vernier Motor and Its Design. *IEEE Trans. Power Appar. Syst.* **1963**, *82*, 343–349. [[CrossRef](#)]
2. Jang, D.-K.; Chang, J.-H. Performance Comparison of PM Synchronous and PM Vernier Machines Based on Equal Output Power per Unit Volume. *J. Electr. Eng. Technol.* **2016**, *11*, 150–156. [[CrossRef](#)]
3. Wu, F.; EL-Refaie, A.M. Permanent Magnet Vernier Machines: A Review. In Proceedings of the 2018 XIII International Conference on Electrical Machines (ICEM), Alexandroupoli, Greece, 3–6 September 2018; pp. 372–378.
4. Kim, B.; Lipo, T.A. Operation and Design Principles of a PM Vernier Motor. *IEEE Trans. Ind. Appl.* **2014**, *50*, 3656–3663. [[CrossRef](#)]
5. Zhao, F.; Lipo, T.A.; Kwon, B. Dual-Stator Interior Permanent Magnet Vernier Machine Having Torque Density and Power Factor Improvement. *Electr. Power Compon. Syst.* **2014**, *42*, 1717–1726. [[CrossRef](#)]
6. Raza, M.; Zhao, W.; Lipo, T.A.; Kwon, B. Performance Comparison of Dual Airgap and Single Airgap Spoke-Type Permanent-Magnet Vernier Machines. *IEEE Trans. Magn.* **2017**, *53*, 1–4. [[CrossRef](#)]
7. Liu, X.; Zhong, X.; Du, Y.; Chen, X. A Novel Triple-Permanent-Magnet-Excited Vernier Machine with Double-Stator Structure for Low-Speed and High-Torque Applications. *Energies* **2018**, *11*, 1713. [[CrossRef](#)]
8. Wei, L.; Nakamura, T. A Novel Dual-Stator Hybrid Excited Permanent Magnet Vernier Machine with Halbach-Array PMs. *IEEE Trans. Magn.* **2021**, *57*, 1–5. [[CrossRef](#)]
9. Zhao, F.; Lipo, T.A.; Kwon, B.-I. Magnet flux focusing design of double stator permanent magnet Vernier machine. In Proceedings of the 19th International Conference on the Computation of Electromagnetic Fields COMPUMAG 2013, Budapest, Hungary, 30 June–4 July 2013; pp. 1–4.
10. Li, D.; Qu, R.; Xu, W.; Li, J.; Lipo, T.A. Design Procedure of Dual-Stator Spoke-Array Vernier Permanent-Magnet Machines. *IEEE Trans. Ind. Appl.* **2015**, *51*, 2972–2983. [[CrossRef](#)]
11. Du, Z.S.; Lipo, T.A. An Improved Rotor Design for Dual-Stator Vernier Ferrite Permanent Magnet Machines. In Proceedings of the 2017 IEEE International Electric Machines and Drives Conference (IEMDC), Miami, FL, USA, 21–24 May 2017; pp. 1–8.
12. Kang, D.H.; Woo, B.C.; Hwang, W. Rotating Electric Device. K.R. Patent KR20190036890A, 5 April 2019.
13. Kang, D.H. Structure of Rotating Electrical Machine with Dual and Multi Air-Gap. PCT/KR2020/014069, 15 October 2020.
14. Hoffer, A.E.; Tapia, J.A.; Petrov, I.; Pyrhönen, J. Design of a Stainless Core Submersible Permanent Magnet Generator for Tidal Energy. In Proceedings of the IECON 2019—The 45th Annual Conference of the IEEE Industrial Electronics Society, Lisbon, Portugal, 14–17 October 2019; IEEE: Piscataway, NJ, USA, 2019; Volume 1, pp. 1010–1015.
15. Duong, M.-T.; Kang, D.-H.; Chun, Y.-D.; Woo, B.-C.; Lee, Y.-S.; Wook, H. Comparison of Dual-Permanent-Magnet-Excited Machines and Surface-Mounted Permanent Magnet Machines in Terms of Force. *Energies* **2019**, *12*, 216. [[CrossRef](#)]